LBL-13015

AN INVESTIGATION ON THE ENHANCEMENT OF THE CRITICAL CURRENT DENSITIES IN BRONZE-PROCESS Nb_3Sn*

M. Hong, I. W. Wu, J. W. Morris, Jr., W. Gilbert,
W. V. Hassenzahl, and C. Taylor

Lawrence Berkeley Laboratory
University of California
Berkeley, California 94720

October 1981

*This work was supported by the Division of High Energy Physics and by the Division of Materials Sciences, U. S. Department of Energy under Contract No. W-7405-ENG-48.

AN INVESTIGATION ON THE ENHANCEMENT OF THE CRITICAL CURRENT DENSITIES IN BRONZE-PROCESS Nb_3Sn

M. Hong*, I. W. Wu**, J. W. Morris, Jr.**, W. ilbert†,
W. V. Hassenzahl†, and C. Taylor†

Lawrence Berkeley Laboratory
University of California
Berkeley, California 94720

INTRODUCTION

Multifilamentary Nb_3Sn A15 superconductors fabricated t the "bronze" process[1,2] or its variants[3,4] have been intensely studied and are strong candidate materials for the construction of magnets to be used for high energy physics and magnetic fusion. In the "bronze" process the A15 compound is formed at the interface between a Nb filament and the Cu-Sn bronze matrix when the composite is at high temperatures. Among the superconducting properties of this system, the one of greatest engineering interest is the critical current density J_c. It is well known that $J_c(H)$ is strongly affected by metallurgical parameters[5,6] such as A15 grain size and Sn content in the A15 layer. There have been many attempts to improve $J_c(H)$ for the "bronze" process. These include the optimization of heat-treatment conditions[7,8] and

*Present address Bell Labs., Murray Hill, NJ 07974
**Materials and Molecular Research Division
†Accelerator and Fusion Research Division

the efforts to find appropriate alloying additions.[9-11] However, the fundamental relationships between processing, microstructure and $J_c(H)$ remain poorly understood.

The work reported here addressed the problem of improving the critical current characteristic of a commercial multifilamentary Nb_3Sn strand[7] by varying its heat treatment. The work was done from the perspective that the critical current characteristic is controlled by the metallurgical state of the reacted layer, which is, in turn, fixed by the processing the wire has undergone. The research was carried out in parallel with metallographic studies[12] which analyzed the microstructure and composition profile within the reacted Nb_3Sn layer as a function of heat treatment. The combined results of metallographic and processing research suggest that it is possible to "engineer" the microstructure of the reacted layer to improve $J_c(H)$. The specific product of the work is a tailored double-aging treatment which introduces a favorable combination of microstructure and composition in the reacted layer and causes a substantial improvement in the critical current characteristic of the strand.

EXPERIMENTAL

The multifilamentary Nb_3Sn strand used in this study was manufactured by AIRCO SUPERCONDUCTORS[7] and has a diameter of 0.7 mm. It contains 2869 (19x151) Nb filaments in a Cu 13 wt% Sn bronze matrix, a tantalum diffusion barrier and stabilizing copper that comprises 64.5% of the cross-sectional area of the strand.

The superconducting A15 phase was formed by heat-treatments at temperatures between 650 and 800°C for various periods of time. Samples were sealed

in quartz tubes under a low pressure argon atmosphere with Titanium rods to minimize contamination.

Critical currents I_c were measured using a standard four-probe technique in transverse applied magnetic fields up to 19 Tesla. The critical current was taken to be that current at which the potential difference across voltage leads spaced 5 mm apart exceeds 1μV, and the overall current density J_c was taken to be the critical current divided by the non-copper area of the strand 0.14 mm^2. Samples for the I_c measurement were in a U-shape with a 25 mm length in the transverse magnetic field.

In the bronze process the Nb_3Sn A15 phase is formed by the diffusion reaction between the Nb core and the Cu-Sn bronze matrix, but the basic thermodynamics and kinetics pertaining to this reaction are inadequately characterized.[13] Due to a lack of quantitative data about the Cu-Nb-Sn ternary equilibrium phase diagram, specifically the detailed shape of the A15 phase range and its tie lines to the Cu-Sn solid solution at various temperatures, it is not possible to predict the Sn concentration across the reacted A15 layer. Therefore, to determine the Sn composition of the A15 layer, we have employed the STEM/EDAX technique to do this micro-chemical analysis.

The microstructure of the reacted wire was characterized through a combination of scanning electron microscopy (SEM), transmission electron microscopy (TEM), and scanning transmission electron microscopy (STEM) as described in Ref. 12. The composition measurements given below were determined from energy dispersive x-ray analysis (EDAX) in the STEM and were computed from the total integrated intensities of the characteristic x-ray peaks of Nb and Sn using the "thin-foil" approximation[14]. The absolute accuracy of the Sn concentration is ~3 at.% in the composition range of interest. The statistical error in determining the relative Sn concentrations at two different points within an

A15 layer is, however, less than 1 at.% Sn. Hence the Sn profiles determined should be reasonably accurate in shape, but may have a small error in absolute value. The spatial resolution of the STEM analysis is limited both by beam size and foil dispersion to ~ 500 Å.

RESULTS AND DISCUSSION

The influence of Aging Temperature on $J_c(H)$

The materials studied in this work were commercial superconductors. Thus the only processing variable available for property improvement was the reaction heat treatment which forms the Nb_3Sn layer on the Nb filament. Previous work[7] on similar strands suggests that the optimum single heat treatment lies in the range 700-800°C and requires a reaction time on the order of two days. The results reported in Ref. 7 are essentially confirmed by the data presented in Fig. 1. Good high field properties resulted from two-day reaction treatments in the range 700-800°C; the best critical current characteristic was obtained after reaction at 730°C. Other heat treatments are included in the figure for comparison.

The Relation Between Aging Temperature, Microstructure, and $J_c(H)$

While two-day heat treatments at temperatures between 700 and 800°C led to reasonable superconducting properties, subsequent metallurgical analysis[12] revealed that major differences occur in the metallurgical state of the Nb_3Sn layer as the aging temperature is varied through this range. At lower temperature the reacted layer has a good structure, but a less desirable composition profile. As the aging temperature rises the structure deteriorates, but the composition profile improves dramatically. It is apparently the balance of

the two effects which causes the maximum in the critical current characteristic near 730°C.

The microstructure of the reacted layer is qualitatively similar for all heat treatments studied. It may be visualized as three concentric cylindrical shells surrounding an unreacted Nb core. The three shells are distinguished by the structure of the A15 grains they contain. They are illustrated in the schematic cross-section shown in Fig. 2. The inner shell consists of large columnar grains which emanate from the Nb core. The central shell contains fine, equiaxed grains which probably form through the break-up of the columnar grains during film growth. The outer shell contains relatively large equiaxed grains which presumably represent coarsening of the finer grains in the interior. Both the overall dimensions of the reacted layer and the relative dimensions of the interior shells depend on heat treatment as shown in Table I.

Since the critical current of the A15 phase is a strong reciprocal function of its grain size[6] the high field portion of the critical current characteristic should be dominated by the central shell of small equiaxed grains. The measured thickness of this shell, 0.8μm, is nearly insensitive to heat treatment temperature for two-day treatments in the range 700-800°C. However, the mean grain size within the shell increases with temperature from ~640 Å at 700°C to ~ 1200 Å at 800°C. The value of J_c at 10T varies roughly with the reciprocal of the grain size, as is expected if the critical current is determined by the substructure of the equiaxed layer. At 14T, on the other hand, the critical current is not simply related to grain size; it is largest for the intermediate grain size associated with the 730°C treatment. This behavior suggests that the composition of the central shell also affects high field properties.

The composition profile across the reacted layer is plotted in Fig. 3 for the three 2-day heat treatments listed in Table I. In each case there is a gradient in the Sn concentration, from a Sn-rich composition at the bronze interface to a Sn-poor concentration at the Nb interface. The composition passed through the stoichiometric value within the fine-grained shell (a phenomena which certainly contributes to the success of the "bronze" process). As the reaction temperature is raised, the reacted layer thickens and the difference between the two end-point compositions narrows. Both effects cause the composition profile to flatten, increasing the thickness of the near-stoichiometric shell within the reacted layer. There is, in addition, an exaggerated flattening of the Sn profile near the stoichiometric composition, which is most pronounced for the 800°C treatment and is responsible for the irregular shapes of the 730°C and 800°C profiles. This effect further increases the near stoichiometric sub-volume of the reacted layer. Since the upper critical field of Nb_3Sn decreases as deviation from chemical stoichiometry increases, a high superconducting current requires a more nearly stoichiometric compound as the field is raised. Because the high-field current will be carried primarily by a sub-shell of the reacted layer whose thickness decreases with increasing field given a composition gradient through the reacted layer, the J_c at high fields decreases more rapidly the sharper the composition gradient in the near-stoichiometric region.

From this perspective it is not surprising that the 700°C treatment, which establishes a sharp concentration gradient through the reacted layer, yields a strand whose critical current decreases rapidly for fields above 12T. The 800°C treatment establishes a relatively flat composition profile at a nearly stoichiometric composition, but an unfavorable microstructure compromises its

high-field properties. The 730°C aging treatment provides a favorable combination of grain size and composition profile and yields the best critical current characteristic for fields in the range 12 to 16T.

Development of An Improved Aging Treatment

The results described in the previous section suggest that the critical current characteristic of the strand is determined by three metallurgical parameters that should be simultaneously controlled: (1) the volume of the fine-grained shell within the reacted layer, which should be as large as possible; (2) the A15 grain size within the fine-grained shell, which should be as small as possible; and (3) the composition profile across the reacted layer, which should be as flat and nearly stoichiometric as possible. Given that the composition of the reacted layer is Sn-rich at the bronze interface and Sn-poor at the Nb interface there is always at least some near-stoichiometric material within an incompletely reacted layer. Hence the composition profile primarily affects $J_c(H)$ at very high fields (>12T in the present case); the lower field properties are largely determined by the grain size and the volume of the fine-grained shell.

These considerations suggest three possible approaches to improve $J_c(H)$: (1) long-time, low-temperature aging with the intent of increasing the thickness of the fine-grained shell and flattening the composition profile while retaining fine grain size; (2) short-time, high-temperature aging with the intent of achieving fine grain size by limiting the time available for grain coarsening while preserving a good composition profile; (3) sequential aging treatments at different temperatures chosen so that one aging establishes a favorable microstructure while the second improves the composition profile. Each of these approaches was explored.

For reasons which appear to be fundamental, neither a longtime, low-temperature nor a short-time, high-temperature aging was successful in improving $J_c(H)$. Increasing the aging time to 8 days at 700°C (Fig. 1, Table I) did result in a small increase in the critical current above 14T, but at substantial cost to the critical current at lower fields. Metallographic analysis showed that the additional heat treatment led to a coarsened grain structure with only a slight increase in the thickness of the fine-grained shell. Raising the temperature to 800°C and decreasing the aging time to 12 hours caused a decrease in $J_c(H)$ at all fields. Parallel metallographic analysis (Table I) revealed a large grain size and a thin central shell.

Given the limitations of modified single aging treatments, a "double-aging" treatment was designed to establish a favorable micro-structure and a favorable composition profile in sequential steps. The microstructure was developed by an initial heat treatment for 2-4 days at 700°C; the composition profile was then improved by an additional aging at 730°C for 2 days. The choice of the 730°C aging temperature was based on earlier results, reported above, which show that 730°C provides a reasonable composition profile without exaggerated grain coarsening. An alternate double-aging proposed in Ref. 8, of 650°C for 16 days plus 800°C for 4 hours was also tried for comparison.

The critical current characteristics of two 700/730°C double-aged specimens are plotted in Fig. 4. These double-aging treatments caused a substantial increase in $J_c(H)$ over the whole range tested. The treatment 700°C, 4 days plus 730°C, 2 days increased J_c by ~40% with respect to the best singleaging treatment. Metallographic analysis of the specimens revealed the source of these good properties. The 700/730°C double-aging treatments provided a relatively thick shell of fine A15 grains as shown in Table II and simultaneously

established a relatively flat Sn profile at a near-stochiometric composition as shown in Fig. 5.

The 650°C, 16 day plus 800°C, 4-hour treatment, on the other hand, gave properties inferior to those of the single-aged specimens. Metallographic analysis showed that the reacted layer had, in this case, both a poor microstructure and a poor composition profile. Further, this reaction sequence is not practical for large magnets.

CONCLUSION

We conclude from the research reported here that the critical current characteristic of bronze-processed multifilamentary Nb_3Sn superconducting wire is largely controlled by three metallurgical parameters: (1) the volume of the finegrained central shell within the reacted A15 layer; (2) the A15 grain size within the fine-grained shell; (3) the composition profile through the reacted layer, which passes from a Sn-rich composition at the bronze interface to a Sn-poor composition at the Nb interface. Each of these features is influenced by heat treatment. Fine grain size is promoted by low temperature reaction while the composition profile is better after reaction at higher temperature. A sequential "double-aging" treatment at 700°C, 4 days plus 730°C, 2 days establishes a superior combination of microstructure and composition and yields critical currents (J_c) which are substantially above the best obtained from single aging treatments over the whole range of fields tested (10-16T).

The results presented here suggest that still better heat treatments can be devised, as the best microstructures obtained in this work are still far from the best that can be imagined. It seems clear that additional research

on metallurgical heat treatment, perhaps coupled with minor changes in manufacturing processes, will lead to important gains in the high-field superconducting properties of multifilamentary Nb_3Sn.

ACKNOWLEDGEMENTS

This work was supported by the Division of High Energy Physics and by the Division of Materials Sciences, U.S. Department of Energy under Contract No. W-7405-ENG-48. The $J_c(H)$ data was obtained at the Francis Bitter National Magnet Laboratory which is supported at M.I.T. by the National Science Foundation. The authors greatly thank J. T. Holthuis, D. R. Dietderich, L. G. Rubin, and B. Brandt for experimental assistance.

REFERENCES

1. A. R. Kaufman and J. J. Pickett, Bull. Am. Phys. Soc. 15, 838 (1970).

2. K. Tachikawa, Proc. of the Third International Cryogenic Engineering Congress, Berlin, Germany, 1970 (Iliffe Science & Technology, Surrey, England, 1971), p. 339.

3. Y. Hashimoto, K. Yoshizaki, and M. Tanaka, Proc. of 5th International Cryogenic Engineering Confernce, Kyoto, Japan (1974), p. 332.

4. M. Suenaga, W. B. Sampson, and T. Luhman, IEEE Trans. on Magn., Vol. MAG. 17, 646 (1981).

5. J. S. Caslaw, Cryogenics 11, 57 (1971).

6. J. D. Livingston, Phy. Status Solid; (a) 44, 295 (1977).

7. P. A. Sanger, E. Adam, E. Ioriatti, and S. Richards, IEEE Trans. on Magn., Vol. MAG. 27, 666 (1981).

8. W. Scnauer and W. Schelb, IEEE Trans. on Magn., Vol. MAG-17, 374 (1981).

9. J. D. Livingston, IEEE Trans, on Magnetics MAG-I4, 611 (1973).

10. H. Sekine ane K. Tachikawa, Appl. Phys. Lett. 35, 472 (1979).

11. K. Tachikawa, T. Tanaka, Y. Yoshida, T. Asano, and Y. Iwasa, IEEE Trans. on Magn. MAG-15, 391 (1979).

12. I. W. Wu, M. Hong, W. V. Hassenzahl, and J. W. Morris, Jr., to be published.

13. J D. Livingston, Filamentary A15 Superconductors, Ed. M. Suenaga and A. F. Clark, 19th Plenum Press, New York, p. 363.

14. J. I. Goldstein, Introduction to Analytical Electron Microscopy, Ed. J. J. Hren, J. I. Goldstein and D. C. Joy, 1979 Plenum Press, New York, p. 83.

Table 1. Comparison of Layer Thickness, Average Grain Size of A15 Phase, and J_c for Various Heat Treatments

Reaction Temperature/Reaction Time	Reacted A 15 Layer Thickness (μm)				Average Equi-axed Grain Size (Å)	J_c(10T) 10^4 A/cm^2	J_c(14T) 10^4 A/cm^2
	Columnar Grains Near Nb Core	Equi-axed Grains	Large Grains Near Bronze	Total			
700 C/ 2 days	0.4	0.8	0.3	1.5	640	5.3	1.7
700 C/ 8 days	0.6	0.9	0.4	1.9	800	3.9	1.9
730 C/ 2 days	0.4	0.8	0.5	1.7	720	5.0	2.0
800 C/ 12 hours	0.6	0.4	0.6	1.6	1090	3.1	0.93
800 C/ 2 days	0.7	0.8	0.8	2.3	1190	3.4	1.2

Table 2. Results of Sequential Heat Treatment

Reaction Temperature/Reaction Time	Reacted A 15 Layer Thickness (μm)				Average Equi-axed Grain Size (Å)	J_c(10T) 10^4 A/cm^2	J_c(14T) 10^4 A/cm^2
	Columnar Grains Near Nb Core	Equi-axed Grains	Large Grains Near Bronze	Total			
730 C/ 2 days	0.4	0.8	0.5	1.7	720	5.0	2.0
700 C/ 2 days + 730 C/2 days	0.4	1.0	0.5	1.9	730	6.2	2.6
700 C/ 4 days + 730 C/ 2 days	0.5	1.2	0.4	2.1	760	6.7	2.8
650 C/ 16 days + 800 C/4 hours	0.4	0.5	0.8	1.7	930	2.9	1.2

FIGURES

XBL NO.	FIG. NO. AND CAPTION
817-6189	Fig. 1. The overall J_c vs. the applied transverse magnetic field for the "bronze" process multifilamentary Nb_3Sn superconductors with single-temperature aging.
818-6372	Fig. 2. Schematic of Nb_3 Sn microstructure near a Nb filament in the bronze process. Columnar grains are adjacent to the Nb and fine grained Nb_3Sn is in the center while coarse grains are close to the bronze, which has been depleted of Sn.
818-6371	Fig. 3. Sn-concentration gradient across the reacted Nb_3Sn A15 layer for two day, single-aging treatments of 700°, 730°, and 800°C.
818-6190	Fig. 4. The overall J_c vs. applied transverse magnetic field for bronze process multi-filamentary Nb_3Sn superconductors with double-aging treatments. (Single aging of 730°C/2 days is used for comparison.)

XBL NO.	FIG. NO. AND CAPTION
817-6193A	Fig. 5. Sn-concentration gradient across the reacted Nb_3Sn A15 layer for two double aging treatments. The large near stoichiometric region in the 700/730°C treatment produces a high critical current in the final conductor.

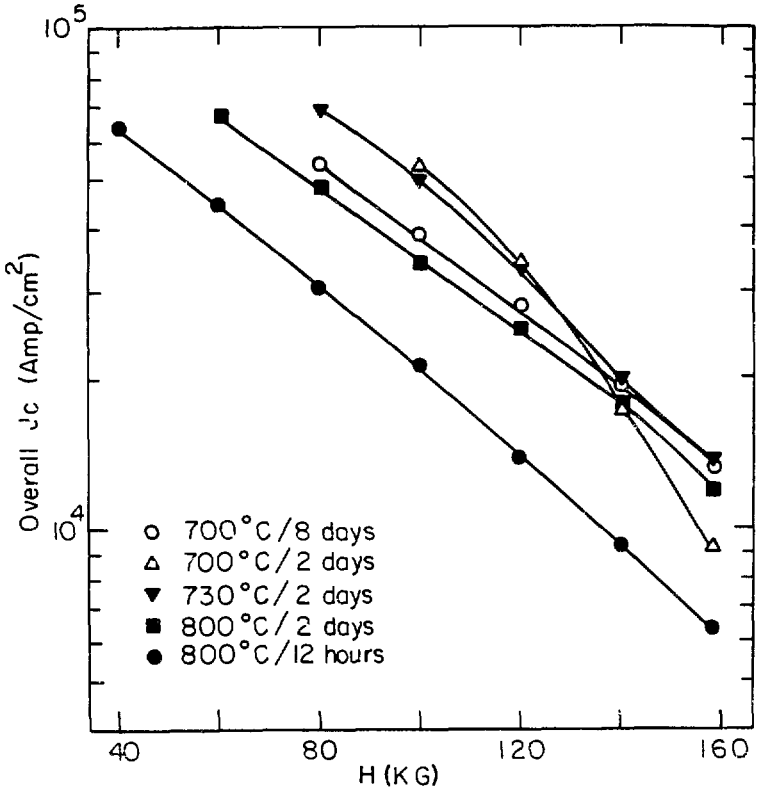

Figure 1

XBL 817-6189

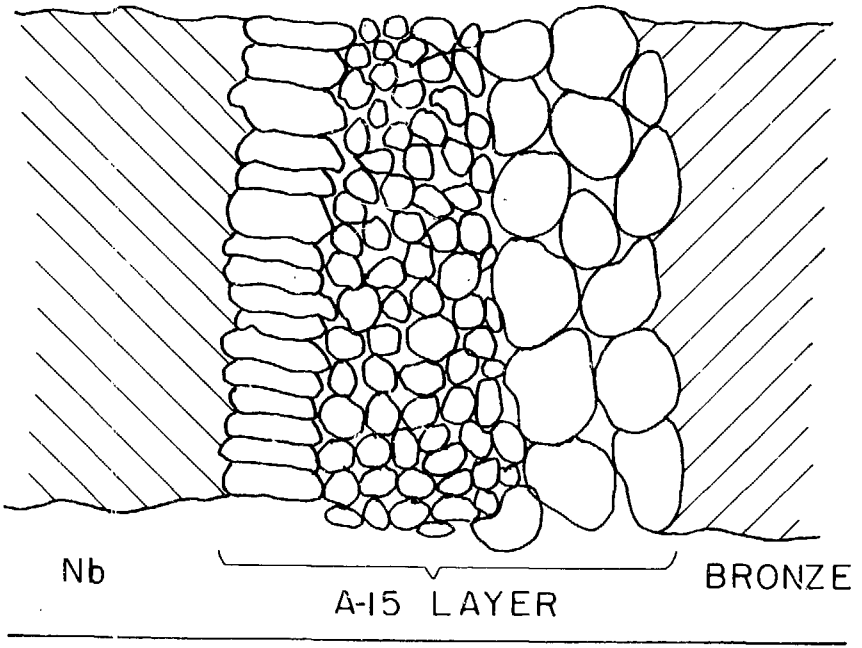

Figure 2

XBL 818-6372

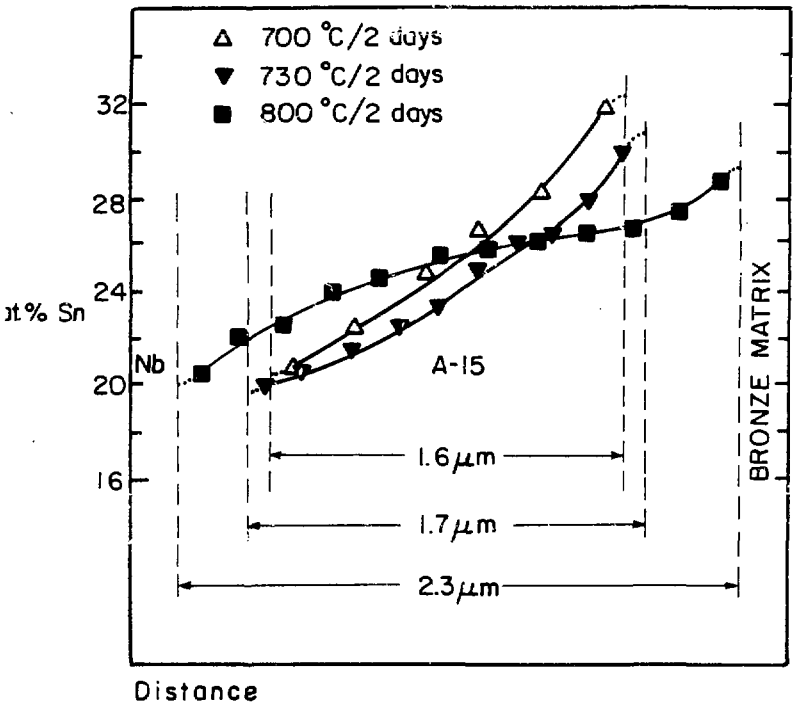

Figure 3

XBL 818-6371

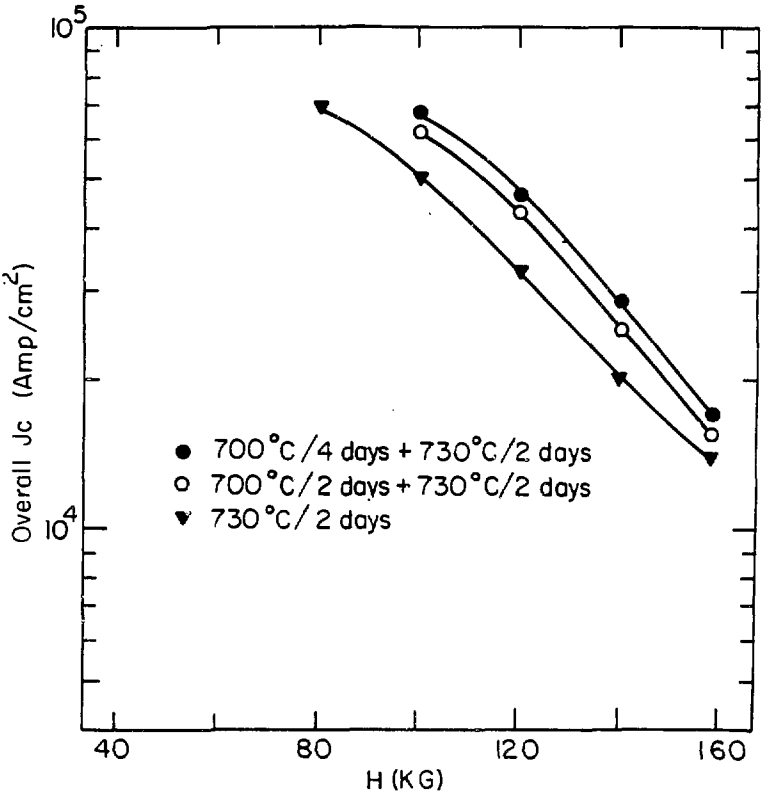

Figure 4

XBL817-6190

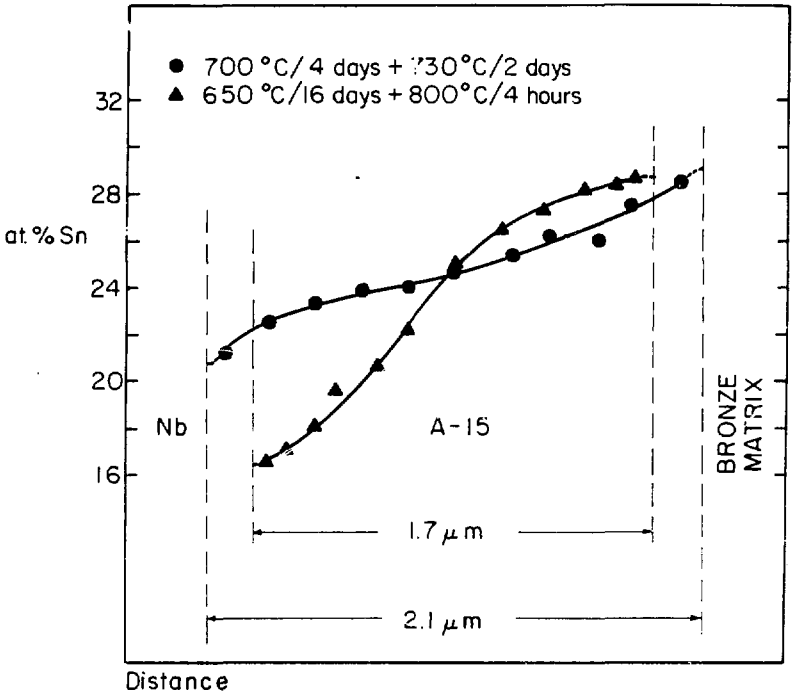

Figure 5

XBL 817 - 6193A